A 0.4–1.2 GHz SiGe Cryogenic LNA for Readout of MKID Arrays

Mohsen Hosseini, Wei-Ting Wong, and Joseph C. Bardin
Department of Electrical and Computer Engineering, University of Massachusetts Amherst, USA
jbardin@engin.umass.edu

Abstract - The design and characterization of a low noise amplifier optimized for the readout of microwave kinetic inductance detectors is described. The work is first motivated through a description of microwave kinetic inductance detectors and a discussion of the requirements for the low-noise amplifiers employed for readout of these devices. Next, the design of a two-stage silicon germanium cryogenic integrated circuit low noise amplifier is presented. The small-signal and large-signal characteristics of the fabricated amplifier are then measured. It is shown that, at a physical temperature of 16 K, the amplifier achieves a gain of greater than 30 dB and an average noise temperature of 3.3 K over the 0.4-1.2 GHz frequency band while dissipating less than 7 mW. Moreover, the wideband compression characteristics are measured it is found that the linearity of the amplifier is sufficient to support frequency domain multiplexed readout of more than 500 detectors.

Keywords — Silicon Germanium, Cryogenic Low Noise Amplifier, Microwave Kinetic Inductance Detector

I. Introduction

Terahertz microwave kinetic inductance detectors (MKIDs) [1] have become popular for use in astronomical applications due to their low noise effective power (NEP) values (e.g., $< 0.4 \,\text{aW}/\sqrt{\text{Hz}}$ at 850 GHz [2] and 1.54 THz [3]) and the relative ease of their readout in comparison to transition edge sensors. An MKID is a planar device that consists of a superconducting resonator, weakly coupled to a transmission line, as shown schematically in Fig. 1. The resonator is typically realized using thin-film superconducting materials and may be implemented with distributed [1] or lumped-element structures [4]. In either case, an MKID is designed to leverage the dependence of a superconductor's kinetic inductance on the density of Cooper pairs in the material; that is, when photons with sufficient energy are absorbed by the superconducting film, they break Cooper pairs, thereby modulating the kinetic inductance, leading to a detectable shift in the series resonant frequency of the coupled MKID $(f_0 \approx 1/2\pi\sqrt{L_{\rm K}(C_{\rm C}+C_{\rm R})})$. The minimum frequency of a photon that can be detected using this technique is determined by the gap energy of the superconducting film (Δ) and is approximated as $f_{\text{MIN}} = 2\Delta/h \approx T_{\text{C}} (73.5 \,\text{GHz/K})$, where h is Planck's constant and $T_{\rm C}$ is the critical temperature of the superconducting film. As such, THz MKIDs typically employ superconducting materials such as Al and TiN, which have critical temperatures in the range of 1-3 K, and the devices are usually cooled to the 100 mK range.

Measured quality factors for MKIDs that are capacitively coupled to a transmission line are on the order of 15,000 [5],

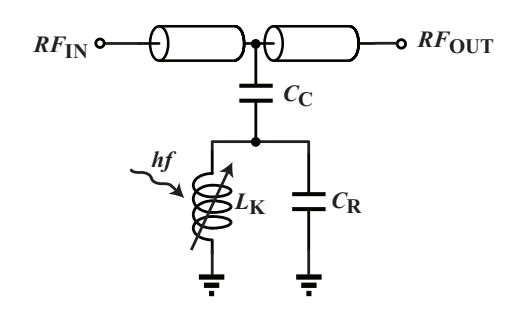


Fig. 1. Schematic diagram of a single MKID. The kinetic inductance $(L_{\rm K})$ is modulated by photon flux, resulting in a shift in the series resonant frequency of the coupled MKID, as observed from the transmission line.

meaning that the fractional frequency range over which any single MKID interacts with the transmission line is well below 0.1%. As the relative value of f_0 can be engineered by varying the relative size of $C_{\rm C}$ and/or $C_{\rm R}$, it is feasible to couple hundreds or even thousands of MKIDs, each with a unique value of $C_{\rm C} + C_{\rm R}$, to a single microwave line.

Readout of the power detected by each pixel can be accomplished using the approach shown in Fig. 2. The readout line is excited by a comb of probe tones, each tuned to the nominal resonant frequency of one of the MKIDs. As the signals pass through the readout line, the readout tones will be modulated due to power dependent frequency shifts in the resonant frequency of the associated MKID. After significant amplification, the amplitude and phase information corresponding to the power absorbed by each MKID is recovered through homodyne detection. Since the information in such a system is carried in the modulation applied to probe tones, SNR is maximized when one uses the strongest possible tones (limited by the power level at which the microwave excitation breaks Cooper pairs [6]). Typical readout tones are in the 1 pW range and, while the phase of each tone can be randomized, the peak to average ratio of the aggregate waveform used to read-out a large MKID array can be well above 10 dB. The cryogenic low noise amplifier (LNA) used for readout must be able to handle such excursions.

In this paper, we present the design and characterization of a SiGe integrated circuit cryogenic LNA that is optimized for integration into a MKID camera that is under currently under development. The final instrument will contain more than 6,000 pixels spread between the 125–170 GHz, 195–245 GHz, and 245–310 GHz bands. We begin by describing the requirements and explaining our design choices. Next we present detailed measurement results. We show that the

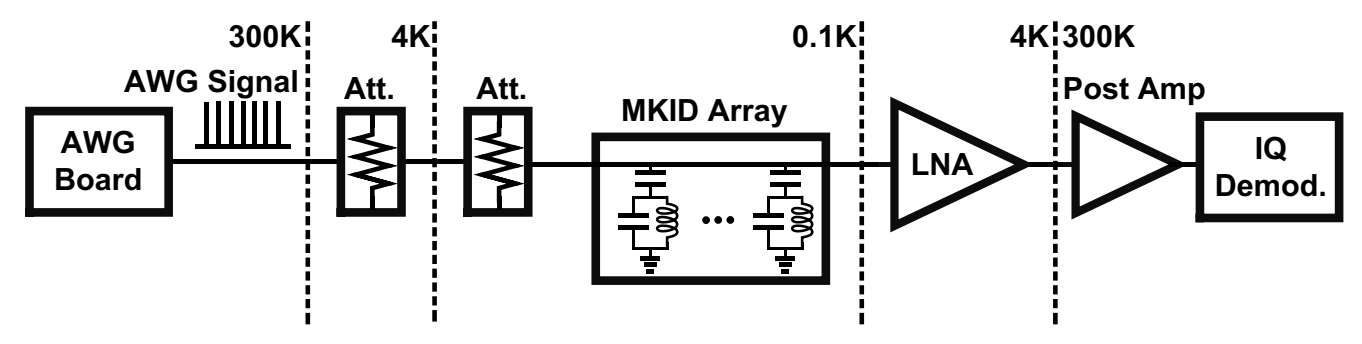


Fig. 2. Block diagram of a typical MKID readout system. The MKID array is excited with a multi-tone stimulus containing one tone per detector. The detectors modulate the tones as their frequencies change in response to incident photons. This modulation is detected using homodyne detection (common LO not shown).

amplifier achieves excellent noise performance while meeting the linearity requirements for multiplexed MKID readout.

II. SYSTEM CONSIDERATIONS AND AMPLIFIER DESIGN

The primary considerations that must be taken into account in specifying a cryogenic LNA for MKID readout are (1) the required probe signal power and frequency band, (2) the impact of LNA noise on overall sensitivity, (3) the available power budget, and (4) the system complexity associated with biasing the cryogenic LNAs. In the case of the camera currently under development, the 6,000 pixels will be interfaced to using a total of 13 readout lines, each operating in the 0.5–1 GHz frequency range. As such, thirteen amplifiers are required and we target a frequency band of 0.4-1.2 GHz to provide margin. The number of detectors coupled to each readout line varies from 450 to 601, so we consider the larger number in setting the linearity requirement. Since the detectors are fabricated out of TiN, the power of each probe tone is assumed to be $-90 \,\mathrm{dBm}$ [7], corresponding to a worst case average power of about $-62 \, dBm$. Thus, the amplifiers should remain linear with input powers in this range.

The second consideration is noise performance. Assuming the amplifier is high gain (i.e., $> 30\,\mathrm{dB}$), its noise contribution will dominate the noise of the overall receiver. It can be shown that the microwave receiver chain contributes a fractional frequency noise of approximately $\sqrt{kT_\mathrm{e}/P_\mathrm{probe}}/Q_\mathrm{C}$ (units: $1/\sqrt{\mathrm{Hz}}$), where T_e is the amplifier noise temperature, P_probe is the microwave probe tone power, and Q_C is the coupling quality factor [5]. While the relative impact of this noise depends strongly on the responsivity of the MKID, we aim to minimize this effect by realizing an amplifier with a noise temperature below 4 K. Such noise performance has previously been demonstrated using SiGe BiCMOS technologies [8], [9].

The power consumption of each amplifier is less constrained as the heat-lift of a typical commercial closed-cycle refrigerator operating at 4 K is on the order of 1 W [10]. Nonetheless, in anticipation of larger-scale arrays, we target a power consumption of less than 7 mW to keep the aggregate DC power consumption around 90 mW.

Finally, we consider the complexity associated with biasing of the amplifier array. The most straightforward

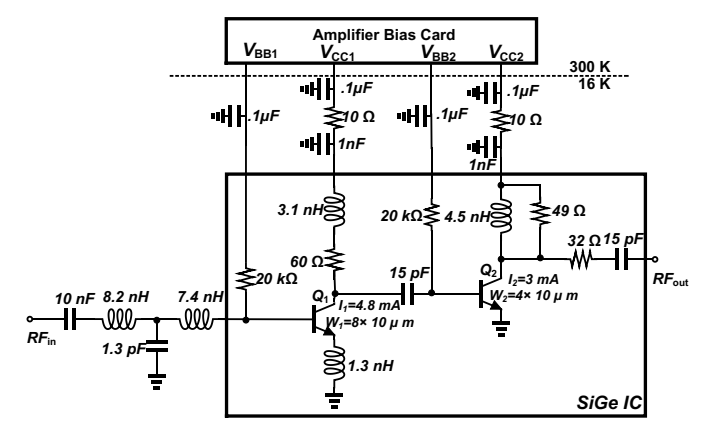


Fig. 3. Schematic of integrated circuit, showing details of the off-chip matching and bias networks.

Table 1. Model parameters extracted at a physical temperature of 18 K. W_E =0.13 μm , $J_{C1,2}$ =0.46, 0.58 $mA/\mu m^2$. A standard hybrid- π model topology has been used [12].

L_E	R_B	R_E	R_C	C_{CB}	C_{CS}	C_{BE}	g_m	τ	β
μm	Ω	Ω	Ω	fF	fF	fF	S	pS	-
80	0.75	0.12	0.65	190	60	436	0.4	0.45	4.6e4
40	1.5	0.24	1.3	95	30	232	0.25	0.47	3.9e4

approach is to employ self-biasing, which has the advantage that it makes single-supply operation feasible. However, there is a significant mismatch between the voltage required at the base ($\approx 1.05 \, \text{V}$ at $16 \, \text{K}$) and that required at the collector ($\approx 300 \, \text{mV}$ at $16 \, \text{K}$) of an HBT operated at cryogenic temperatures [11]. As such, we have avoided this approach and opted for independent control of each base voltage. To ease the challenge of generating and distributing a large number of bias voltages to the 13 amplfiers, we have designed a servo-bias system to maintain constant collector current while operating from a low collector supply voltage. The bias circuitry is further described in Section III.

A two-stage integrated circuit amplifier was designed using small-signal models extracted at a physical temperature of 15 K for HBTs from the ST BiCMOS9MW technology platform. A schematic diagram of the designed amplifier appears in Fig. 3. The current density of Q_1 was set to approximately $0.48\,\mathrm{mA}/\mu\mathrm{m}^2$ to minimize T_MIN in the

0.4-1.2 GHz frequency range and the transistor periphery was set to $8 \times 10 \,\mu\text{m} \times 0.13 \,\mu\text{m}$, to bring the optimum generator resistance at the upper part of the band near 50Ω . The emitter degeneration inductance and the L-R network loading the first-stage transistor were designed to bring the real-part of the input resistance close to that of Γ_{OPT} . While it is feasible to realize high performance cryogenic low noise amplifiers with on-chip input matching networks, here we chose to use an off-chip input matching network to enable re-tuning as needed. The input matching network consists of a third-order ladder network, which has been optimized as a trade-off between noise and power matching over the 0.4-1.2 GHz frequency range. The second-stage was designed to flatten the gain and provide an output match. The second-stage transistor was sized as $4 \times 10 \,\mu\text{m} \times 0.13 \,\mu\text{m}$ and biased at a current density of approximately $0.58\,\mathrm{mA}/\mu\mathrm{m}^2$. The output matching network employs resistive padding to achieve a broadband impedance match to $50\,\Omega$. Simulations of the amplifier were carried-out using the HBT model parameters provided in Table 1 and predict $S_{11} < -7 \,\text{dB}$, $S_{22} < -13$, $S_{21} > 30$, and $T_e < 4$ over the entire 0.4-1.2 GHz frequency range.

III. RESULTS

The low noise amplifier was fabricated using the ST BiCMOS9MW technology platform. The chip was packaged in a housing for characterization, (see Fig. 4). The input matching network was realized using air-core inductors and wirebondable silicon metal-insulator-semiconductor capacitors. The 1 nF bypass capacitors in Fig. 3 were realized using wirebondable high-density silicon MOS capacitors, which can be seen in Fig. 4. In addition to the amplifier module, a custom room-temperature bias board was designed and fabricated. This board functions to provide regulated voltages for the collectors while servoing the base voltages for constant collector currents. While this is not necessary for the operation of a single amplifier, as described in Section II such a standalone bias network is essential from a system perspective.

After assembly, the amplifier was mounted in a closed-cycle cryostat for characterization at a physical temperature of 16 K. These measurements were carried-out in a two-channel cryostat, with one channel used for scattering parameters measurements and the second used for cold attenuator [13] based noise measurements. The amplifier was biased at $V_{C1} = 0.85 \,\text{V}$, $I_{C1} = 4.8 \,\text{mA}$, $V_{C2} = 0.85 \,\text{V}$, and $I_{C2} = 3 \,\mathrm{mA}$. The results of these measurements appear along with simulation results in Fig. 5. The gain and noise performance aggrees quite well with simulation. The amplifier has a gain greater than 30 dB over the 0.4-1.2 GHz frequecy range and its average noise temperature over the 0.5-1 GHz and 0.4-1.2 GHz frequency range is 3.1 K and 3.3 K, respectively. The measured input and output return losses differ some from simulation, which may be explained by the difference in reference plane, as the measurement included long coaxial cables within the cryostat. Nonetheless,

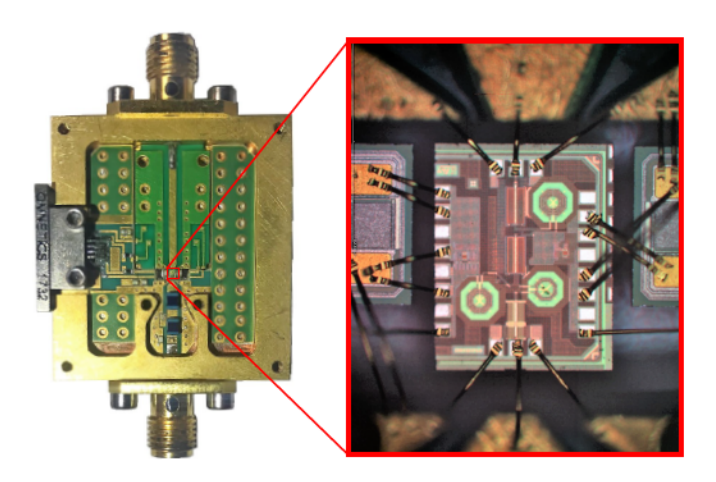


Fig. 4. Photographs of the module and wirebonded IC. The chip dimensions are 1.1 mm \times 1.2 mm.

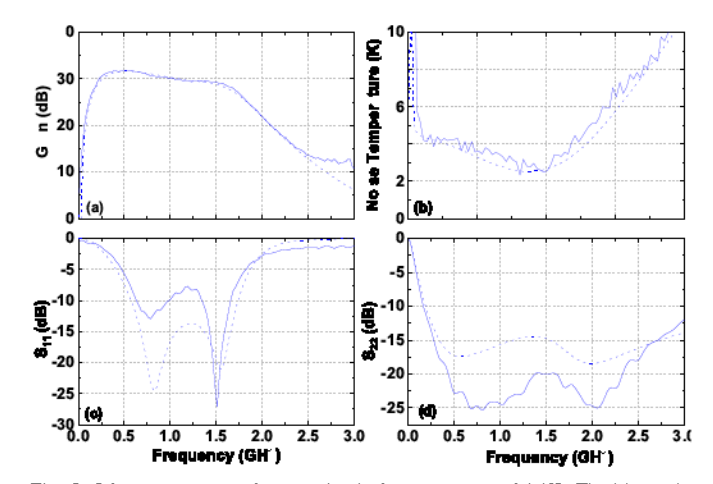


Fig. 5. Measurement results at a physical temperature of 16 K. The bias point for these measurements was $V_{\rm CC1}=V_{\rm CC2}=0.85$ V, $I_{\rm CC1}=4.8$ mA, and $I_{\rm CC2}{=}3$ mA. (a) Gain, (b) Noise Temprature, (c) S_{11} , and (d) S_{22} . Solid lines are measurement data whereas dashed lines are simulation.

the measured input and output return losses are believed to be sufficient for this application.

Next, we measured the compression characteristics of the device to evaluate its suitability for use in a multiplexed MKID readout system. These measurements were carried-out using the test setup shown in Fig. 6, with both CW and multi-tone stimuli. For the multi-tone measurement, we employed a frequency comb consisting of 560 sinusoidal tones spanning the frequency range of 0.4-0.85 GHz, as shown in Fig. 7. This frequency range was chosen to align with the filters shown in Fig. 6. Results of the CW compression measurements are compared to those of the multi-tone measurement in Fig. 8 for a bias point of $V_{CC1} = 0.7 \text{ V}$, $I_{CC1} = 4.8 \text{ mA}$, $V_{\rm CC2}=0.5$ V, and $I_{\rm CC2}=3$ mA ($P_{\rm DC}=4.9$ mW). In all cases, the input-referred 1 dB compression point was found to be greater than $-53 \, dBm$. Based on these results, it appears that the amplifier should be able to amplify the required spectrum without introducing significant distortion.

The amplifier is compared to other recent SiGe cryogenic integrated circuit LNAs in Table 2. While the bandwidth of the

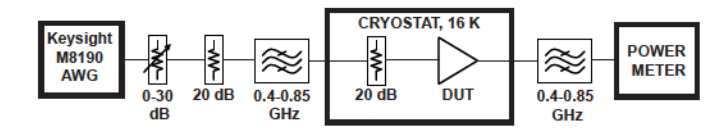


Fig. 6. Test setup used to characterize compression characteristics of the LNA. For CW measurements, the arbitrary waveform generator was replaced by a CW generator.

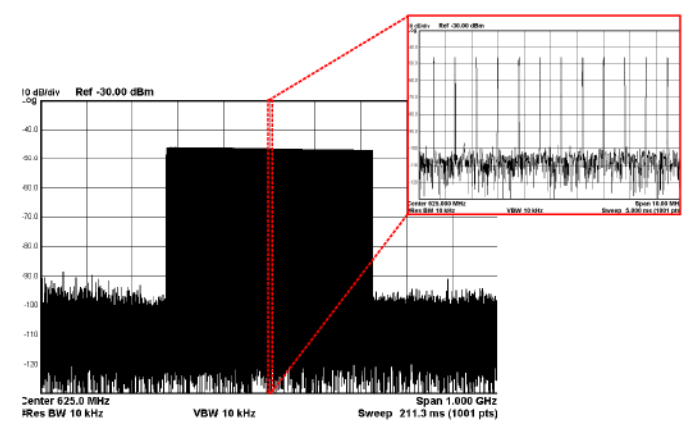


Fig. 7. Spectrum of multi-tone stimulus. The signal consists of 560 evenly spaced tones spanning the frequency range of 0.4-0.85 GHz.

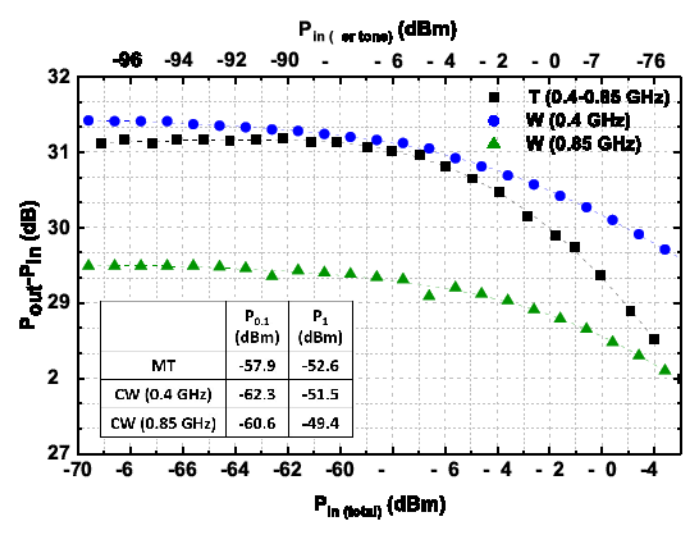


Fig. 8. Measured compression characteristics for a CW (Blue=0.4 GHz and green=0.85 GHz) and a multi-tone stimulus (Black). The upper x-axis scale corresponds to the input power per-tone for the multi-tone stimulus, which is expected to be $\leq -90 \, \mathrm{dBm}$ for the actual system.

reported amplifier is lower than the other examples, it offers an excellent combination of low noise, high gain, and moderate power consumption.

IV. CONCLUSION

A cryogenic low noise amplifier optimized for the readout of multiplexed MKID arrays has been presented and the measured results confirm that the device meets the system specifications required by an MKID camera that is currently in development. Future work should involve characterization

Table 2. Comparison with state-of-the-art SiGe cryogenic LNAs ICs.

Reference	Frequency	T_{ε} (Avg)	P_{DC}	Gain	T_{α}
-	GHz	۰K	mW	₫B	۰K
[14]	0.1-5	5	20	30	15
[9]	0.3-3	2.8	32	22	16
[15]	0.3-5	12	2	15	4
[15]	0.3-8	9	8.2	18	19
This Work	0.4-1.2	3.3	6.6	30	16

of the amplifier with an MKID array as well as integration of a full amplifier array into the complete instrument.

ACKNOWLEDGMENT

The authors would like to thank Prof. Grant W. Wilson and Prof. Phillip Mauskopf for their outstanding advises. We also thank ToITEC project members for their help.

REFERENCES

- P. K. Day, H. G. LeDuc, B. A. Mazin, A. Vayonakis, and J. Zmuidzinas, "A broadband superconducting detector suitable for use in large arrays," *Nature*, vol. 425, no. 6960, p. 817, 2003.
- [2] L. Ferrari, O. Yurduseven, N. Llombart, S. J. Yates, J. Bueno, V. Murugesan, D. J. Thoen, A. Endo, A. M. Baryshev, and J. J. Baselmans, "Antenna coupled MKID performance verification at 850 GHz for large format astrophysics arrays," *IEEE Transactions on Terahertz Science and Technology*, vol. 8, no. 1, pp. 127-139, 2018.
- [3] P. de Visser, J. Baselmans, J. Bueno, and T. Klapwijk, "Demonstration of an NEP of 3.8× 10⁻¹⁹ W/Hz^{1/2} at 1.54 THz in multiplexible superconducting microresonator detectors," in *Infrared, Millimeter, and Terahertz waves (IRMMW-THz)*, 2014 39th International Conference on. IEEE, 2014, pp. 1-2.
- [4] S. Doyle, P. Mauskopf, J. Naylon, A. Porch, and C. Duncombe, "Lumped element kinetic inductance detectors," *Journal of Low Temperature Physics*, vol. 151, no. 1-2, pp. 530-536, 2008.
- [5] P. Mauskopf, "Transition edge sensors and kinetic inductance detectors in astronomical instruments," *Publications of the Astronomical Society* of the Pacific, vol. 130, no. 990, p. 082001, 2018.
- [6] P. De Visser, S. Withington, and D. Goldie, "Readout-power heating and hysteretic switching between thermal quasiparticle states in kinetic inductance detectors," *Journal of Applied Physics*, vol. 108, no. 11, p. 114504, 2010.
- [7] J. Hubmayr, J. Beall, D. Becker, H.-M. Cho, M. Devlin, B. Dober, C. Groppi, G. C. Hilton, K. D. Irwin, D. Li et al., "Photon-noise limited sensitivity in titanium nitride kinetic inductance detectors," Applied Physics Letters, vol. 106, no. 7, p. 073505, 2015.
- [8] J. C. Bardin, "Silicon-germanium heterojunction bipolar transistors for extremely low-noise applications," Ph.D. dissertation, California Institute of Technology, Pasadena, California, May 2009.
- [9] S. W. Chang and J. C. Bardin, "A wideband cryogenic SiGe LNA MMIC with an average noise temperature of 2.8 k from 0.3-3 GHz," in 2017 IEEE MTT-S International Microwave Symposium (IMS), June 2017, pp. 157-159.
- [10] "PT410 cryorefrigerator capacity curve," Cryomech, Syracuse, NY.
- [11] S. Montazeri, W. T. Wong, A. H. Coskun, and J. C. Bardin, "Ultra-low-power cryogenic SiGe low-noise amplifiers: Theory and demonstration," *IEEE Transactions on Microwave Theory and Techniques*, vol. 64, no. 1, pp. 178-187, Jan 2016.
 [12] J. C. Bardin and S. Weinreb, "Experimental cryogenic modeling and
- [12] J. C. Bardin and S. Weinreb, "Experimental cryogenic modeling and noise of SiGe HBTs," in *Microwave Symposium Digest*, 2008 IEEE MTT-S International. IEEE, 2008, pp. 459-462.
- [13] J. Fernandez, "A noise-temperature measurement system using a cryogenic attenuator," TMO progress report, vol. 15, pp. 42–135, 1998.
 [14] J. C. Bardin and S. Weinreb, "A 0.1-5 GHz cryogenic SiGe MMIC
- [14] J. C. Bardin and S. Weinreb, "A 0.1-5 GHz cryogenic SiGe MMIC LNA," IEEE Microwave and Wireless Components Letters, vol. 19, no. 6, pp. 407-409, June 2009.
- [15] D. Russell and S. Weinreb, "Low-power very low-noise cryogenic SiGe IF amplifiers for terahertz mixer receivers," *IEEE Transactions* on Microwave Theory and Techniques, vol. 60, no. 6, pp. 1641–1648, June 2012.